Journal of Orthopaedic Surgery and Research

RESEARCH ARTICLE

Open Access

Biomechanical comparison of femoral neck anti-rotation and support system versus femoral neck system for unstable pauwels III femoral neck fractures

Taiyou Wang[1,2†], Guangjian Wang[1,3†], Fukang Zhu[1,2] and Bo Qiao[1,2*]

Abstract

Background The optimal treatment method for managing unstable Pauwels III femoral neck fractures remains undetermined. The aim of this study was to compare the biomechanical properties of two types of Femoral Neck Anti-rotation and Support System (FNAS) and a Femoral Neck System (FNS) in unstable Pauwels III femoral neck fractures.

Methods Eighteen synthetic femoral models were implanted with one of three fixation devices: FNS, FNAS I, or FNAS II. An unstable Pauwels III (OTA/AO 31-B2.3) femoral neck fracture was simulated using a custom-made needle and osteotomy guide. Torsion and axial compression loading tests were conducted, and the torque, torsion angle, load to failure, displacement, and stiffness values were recorded.

Results FNAS II exhibited significantly higher torsional stiffness (0.67 ± 0.10 Nm/°) compared to FNAS I (0.52 ± 0.07 Nm/°, $P = 0.01$) and FNS (0.54 ± 0.07 Nm/°, $P = 0.005$). FNS demonstrated significantly greater mean axial stiffness (239.24 ± 11.38 N/mm) than both FNAS I (179.33 ± 31.11 N/mm, $P = 0.005$) and FNAS II (190.07 ± 34.11 N/mm, $P = 0.022$). FNAS I (302.37 ± 33.88 N/mm, $P = 0.001$) and FNAS II (319.59 ± 50.10 N/mm, $P < 0.001$) showed significantly higher initial axial stiffness compared to FNS (197.08 ± 33.68 N/mm). Both FNAS I and II improved resistance to deforming forces at a load level before approximately 1000 N, which is sufficient to withstand the load from most daily life activities. No significant differences were observed in compression failure load among the groups. The failure patterns at the point of failure included the pull-out of the distal locking screw and reverse oblique intertrochanteric femur fracture for FNS, while for FNAS I and II, the failures were characterized by a cleft on the calcar femorale and a decrease in the load–displacement curve.

Conclusions In unstable Pauwels III femoral neck fractures, the FNAS II enhances stability and is easier to manage for reoperation. The results of the current study support the potential of FNAS II as an alternative option for treating unstable Pauwels III femoral neck fractures in young individuals.

†Taiyou Wang and Guangjian Wang contributed equally to this work.

*Correspondence:
Bo Qiao
qiaobo1985@163.com

Full list of author information is available at the end of the article

Keywords Biomechanics, Femoral neck fractures, Femoral Neck anti-rotation and support system, Femoral Neck System

Background

By 2050, over half of global hip fractures are expected to occur in Asia [1], with approximately 50% of them being femoral neck fractures [2]. Femoral neck fractures in young patients are usually secondary to high-energy trauma, resulting in a vertical fracture [3]. Although cannulated screws fixation is the standard treatment for unstable vertical femoral neck fractures in young patients [4], it poses significant challenges and economic burdens due to high rates of complications such as avascular necrosis of the femoral head, nonunion, and internal fixation failure [5].

To address these issues, the Femoral Neck System (FNS) was developed, integrating the advantages of minimally invasive implantation, rotational stability, and sliding compression. However, a recent meta-analysis [6] suggested that, despite the FNS showing faster union rates and less neck shortening in young patients with femoral neck fractures, the rates of complications such as implant failure, non-unions, and avascular necrosis remained similar to those treated with cannulated screws. Moreover, the FNS did not demonstrate significantly greater superiority than cannulated screws in terms of final functional status or pain relief.

Ideal implants should provide buttress and resistance in both the calcar femorale and Ward's triangle areas, while also preventing head rotation to enhance stability during fracture treatment [7]. Therefore, based on this principle, we designed a novel angle fixed device termed as a Femoral Neck Anti-Rotation and Support System. The FNAS consists of a barrel, bolt, anti-rotation screw, and distal locking screw (Fig. 1). FNAS I and II have differences in the angle between the bolt and the anti-rotation screw, with FNAS I being 7.5° and FNAS II being 10°. The anti-rotation screw passes out from beneath the barrel to buttress the calcar femorale and Ward's triangle while the locked combination of the bolt and anti-rotation screw restricts rotation around the head-neck axis.

The purpose of the study was to assess the biomechanical properties of two types of FNAS and a FNS in unstable Pauwels III femoral neck fractures. We hypothesize that by increasing the locking angle between the bolt and the anti-rotation screw, and by providing a buttress in the calcar femorale and Ward's triangle, FNAS II offers a biomechanical advantage over FNS in terms of rotational stability and axial stiffness.

Methods

Specimen preparation

A total of 18 right synthetic femur models (Model 2200, Synbone, Zizers, Switzerland) were utilized for this biomechanical analysis. The power analysis, using findings from the pilot study (alpha=0.05, effect size=1.0, power=0.8), indicated that at least 5 models per group are needed to detect significant differences. The selected synthetic femur models mimic the mechanical properties of young individuals, who are typically victims of Pauwels III fractures [8]. Additionally, synthetic femurs show significantly less variability compared to cadaveric femurs [3]. All samples were assigned to one of three test groups (n=6). Group A received FNS fixation (95 mm, Forwos Medical, Chongqing, China), group B received FNAS I fixation (95 mm, locking angle at 7.5°, Forwos Medical, Chongqing, China), while group C received treatment with FNAS II (95 mm, locking angle at 10°, Forwos Medical, Chongqing, China).

Osteotomy and surgical technique

To ensure comparable implant placement and standardized fractures in all specimens, a 3D-printed needle and osteotomy guide were designed (Fig. 2). Synthetic femur models were pre-drilled through the needle guide. After guide-pin insertion, FNS, FNAS I and FNAS II were respectively inserted into the models. Then, implants were removed to perform osteotomy through saw guide. To simulate unstable Pauwels III fracture (OTA/AO 31-B2.3, Pauwels angle=70°), two cuts were made with a hacksaw to remove a median wedge from the femoral neck, with the first cut executed at a 70° angle, according to the classification of a Pauwels III fracture type [9]. Subsequently, an 18° wedge at the first cut's proximal end was removed [10]. To prevent head rotation while inserting the implants, the fractured femur model was secured within a custom-made mold. After re-inserting the implants, radiography was performed to confirm their standard placement (Fig. 3). Before the biomechanical test, each specimen underwent distal shortening to ensure a length of 20 cm.

Biomechanical testing

Torsion testing was conducted using a torsion testing machine (TMT201, SUST, Zhuhai, China). A custom-made jig secured the sample with set screws, aligning the axis of the femoral neck with that of the testing machine (Fig. 4). A non-destructive load was selected to avoid affecting subsequent tests [11]. Torque was applied at 0.5°/s until achieving a 10° rotation, indicative of a

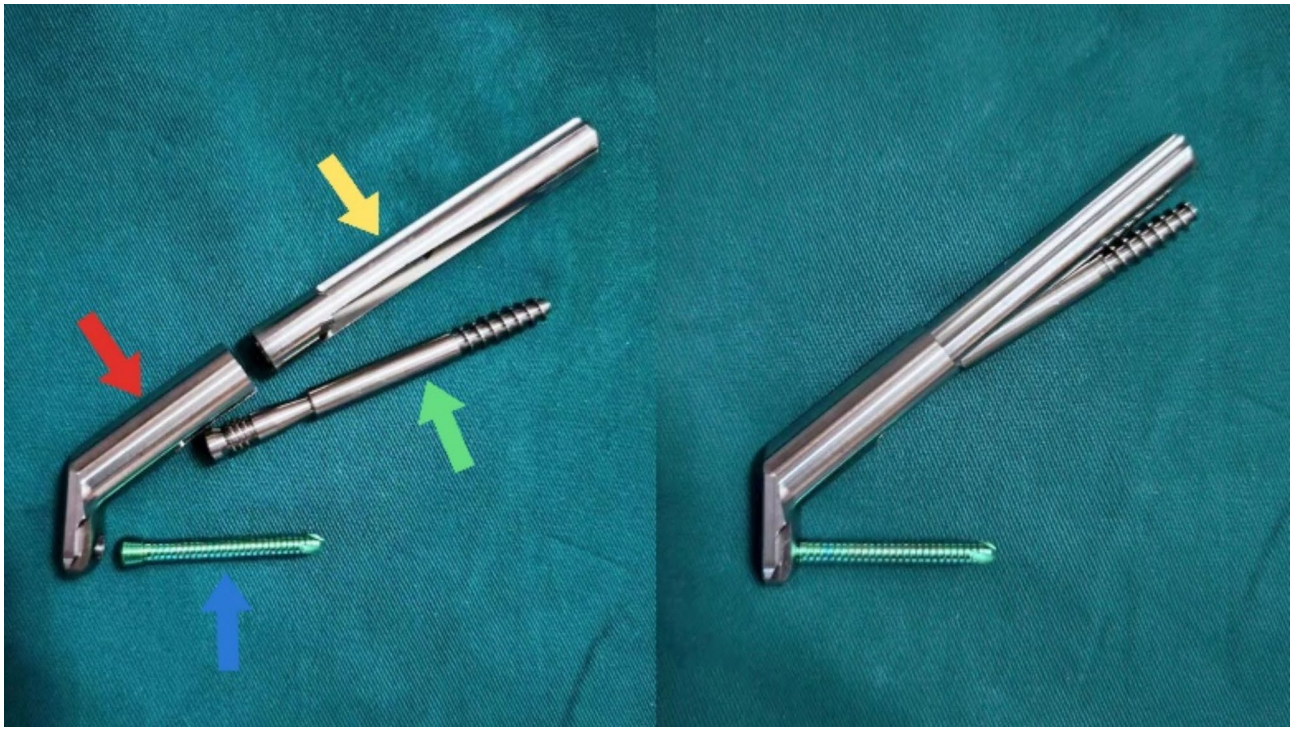

Fig. 1 Femoral Neck Anti-rotation and Support System that consists of a barrel (red arrow), bolt (yellow arrow), anti-rotation screw (green arrow), and distal locking screw (blue arrow)

clinically significant risk of non-union [12]. Data of torque and torsion angle were recorded and torsional stiffness was calculated from the slope of the torque-angle curve during loading.

Then, axial compression loading testing was performed using a material testing machine (CMT5105, SUST, Zhuhai, China). During compression, specimens were mounted vertically with a 16° adduction to simulate the hip contact force in vivo [13]. An acetabulum-shaped cap was placed proximally on the femoral head for transmitting the compression load (Fig. 4). Each specimen was preloaded to 100 N to eliminate the gap between implants and the femoral model. A static loading approach, incrementing to 500 N at a ramp rate of 3 mm/s, was employed to evaluate the initial axial stiffness. Compression loading then continued to increase until one of the defined internal fixation failure criteria was achieved: (1) fracture of the femoral model or the implant; (2) a sudden decrease in load resistance observed on the load–displacement curve; (3) screw cut-out or pullout; (4) 15 mm relative axial displacement of the machine actuator; (5) reaching 4000 N axial load. The failure mode, failure load, and failure displacement were recorded. Initial and mean axial stiffness were calculated from the slope of the load–displacement curve during loading.

Statistical analysis

Statistical analysis is performed using SPSS software (version 25.0, IBM, New York, USA). The Shapiro–Wilk test is applied to assess the normality of data. Once normality is confirmed, the differences in torsional stiffness, initial axial stiffness, mean axial stiffness, and failure load among the three groups are examined using a one-way analysis of variance (ANOVA), with Bonferroni post hoc tests for multiple comparisons. P of 0.05 is selected to define statistical significance.

Results

In the biomechanical testing of three fixation methods, there were statistically significant differences in torsional stiffness, initial axial stiffness, and mean axial stiffness (Table 1). The torsional stiffness of the FNAS II group was 0.67±0.10 Nm/°, significantly higher than that of the FNS group at 0.54±0.07 Nm/° (P=0.010) and the FNAS I group at 0.52±0.07 Nm/° (P=0.005) (Fig. 5). Regarding initial axial stiffness, the FNAS I group measured at 302.37±33.88 N/mm (P=0.001) and the FNAS II group at 319.59±50.10 N/mm (P<0.001), both significantly higher than the FNS group at 197.08±33.68 N/mm. For mean axial stiffness, the FNS group was 239.24±11.38 N/mm, significantly higher than both the FNAS I group at 179.33±31.11 N/mm (P=0.005) and the FNAS II group at 190.07±34.11 N/mm (P=0.022). Compression failure load was 1933.87±220.69 N for FNS group,

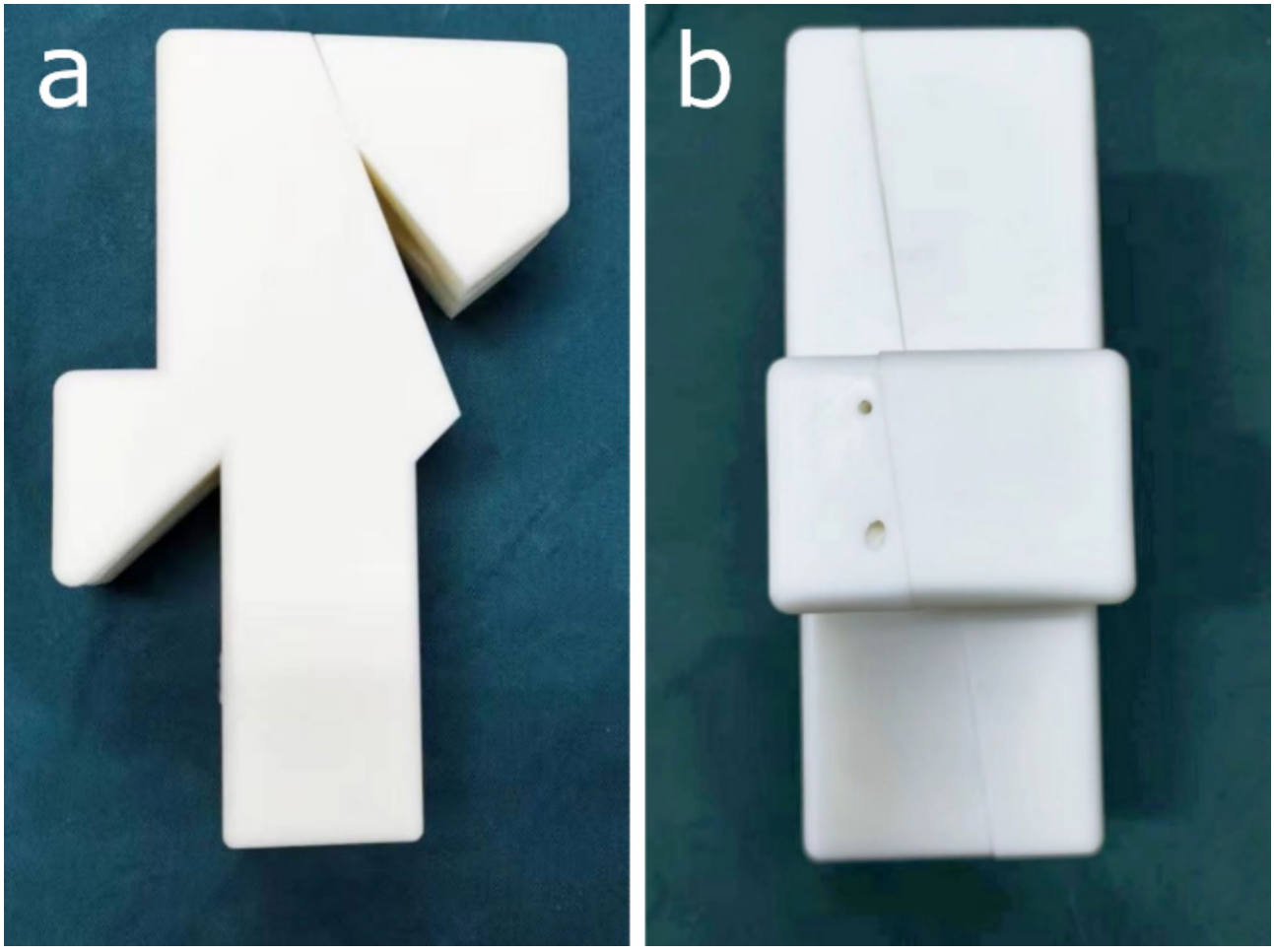

Fig. 2 3D-printed needle and osteotomy guide. (**a**) anteroposterior view; (**b**) lateral view

1762.43±171.16 N for FNAS I group, 1660.52±308.19 N for FNAS II group, with no statistical significances (P=0.172). During the axial compression tests, a turning point at approximately 800 to 1100 N load was observed in the load–displacement curves of the constructs for both FNAS groups (Fig. 5). There were no significant differences in initial (P>0.999) and mean axial stiffness (P>0.999) between the FNAS I and FNAS II groups.

The failure patterns of the three fixation methods were different, and the typical characteristics of the failure patterns are shown in Fig. 6. In the FNS group, internal fixation failure was observed in 5 cases as the pullout of the distal locking screw, while 1 case of catastrophic failure occurred, which was a reverse oblique intertrochanteric femur fracture. In the FNAS I group, 5 cases exhibited a cleft of the calcar femorale, and 1 case reached the failure criteria with a sudden decrease in load resistance observed on the load–displacement curve. For the FNAS II group, 3 cases showed a cleft of the calcar femorale, and the other 3 cases demonstrated a decrease in the load–displacement curve (Table 2).

Discussion

In the present study, the biomechanical properties of the FNAS and the FNS for unstable Pauwels III femoral neck fractures are investigated through biomechanical tests. The results reveal that FNAS II exhibits advantages of anti-rotation function compared to the other two groups. Both FNAS I and II show advantages in axial compression before 1000 N load level. Additionally, the failure modes of FNAS I and II are more manageable for reoperation compared to FNS.

Poor rotational stability is associated with the most common failure modes of a hip fracture fixation device and cut-out usually follows a rotational movement of the femoral head fragment [14, 15]. It is crucial to enhance the anti-rotational capability of the implants for reducing the incidence of complications. The results show that the FNAS II group exhibits highest torsional stiffness while FNS and FNAS I group do not show significant differences. Torsional stiffness (K_t) is a structural characteristic that indicates the degree of twisting under a given torque, describing the structure's ability to resist torsional forces. It is typically represented as the ratio of torque (T)

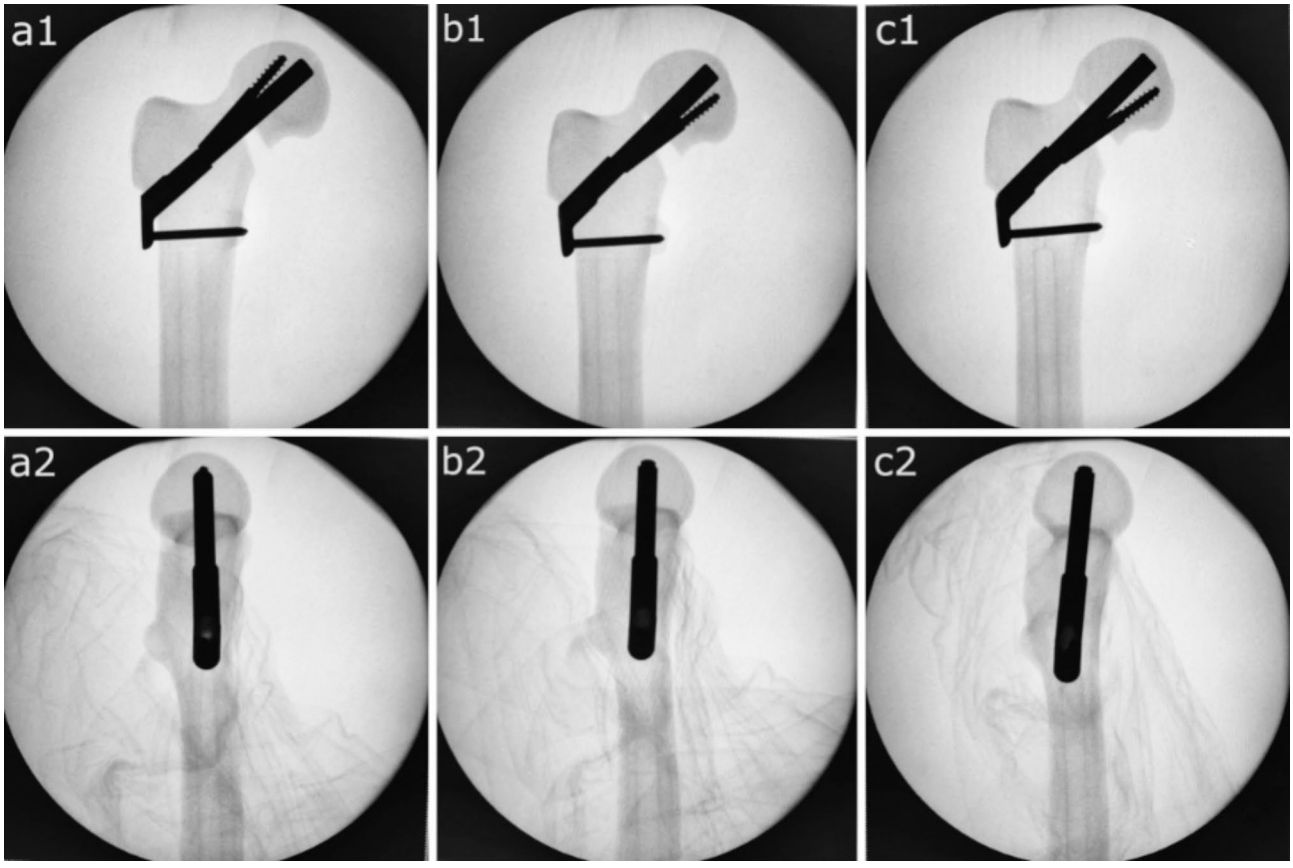

Fig. 3 Fluoroscopic views of three fixation methods. (**a1**) anteroposterior view of FNS; (**a2**) lateral view of FNS; (**b1**) anteroposterior view of FNAS I; (**b2**) lateral view of FNAS I; (**c1**) anteroposterior view of FNAS II; (**c2**) lateral view of FNAS II

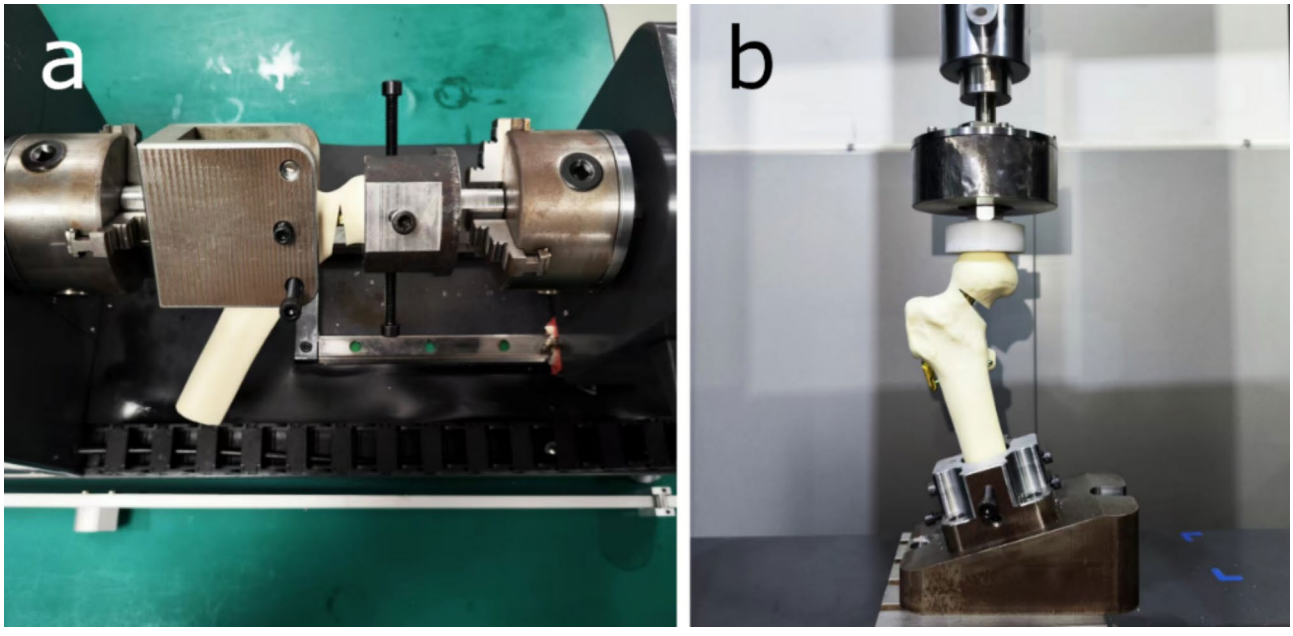

Fig. 4 Biomechanical testing. (**a**) torsion testing; (**b**) axial compression loading testing

Table 1 Biomechanical test results of three fixation methods

Group	Torsional stiffness (Nm/°)	Initial axial stiffness (*N*/mm)	Mean axial stiffness (*N*/mm)	Load to failure (*N*)
FNS	0.54±0.07	197.08±33.68	239.24±11.38	1933.87±220.69
FNAS I	0.52±0.07	302.37±33.88[a***]	179.33±31.11[a**]	1762.43±171.16
FNAS II	0.67±0.10[a**,b**]	319.59±50.10[a***]	190.07±34.11[a*]	1660.52±308.19
F	8.829	16.525	8.126	1.986
P	0.003	< 0.001	0.004	0.172

a, vs. Group FNS; b, vs. Group FNAS I; * means $p<0.05$, ** means $p<0.01$, *** means $p<0.001$

Values are presented as mean ± standard deviation

Different letters (a, b) indicate significant differences in the same column by Bonferroni post hoc test

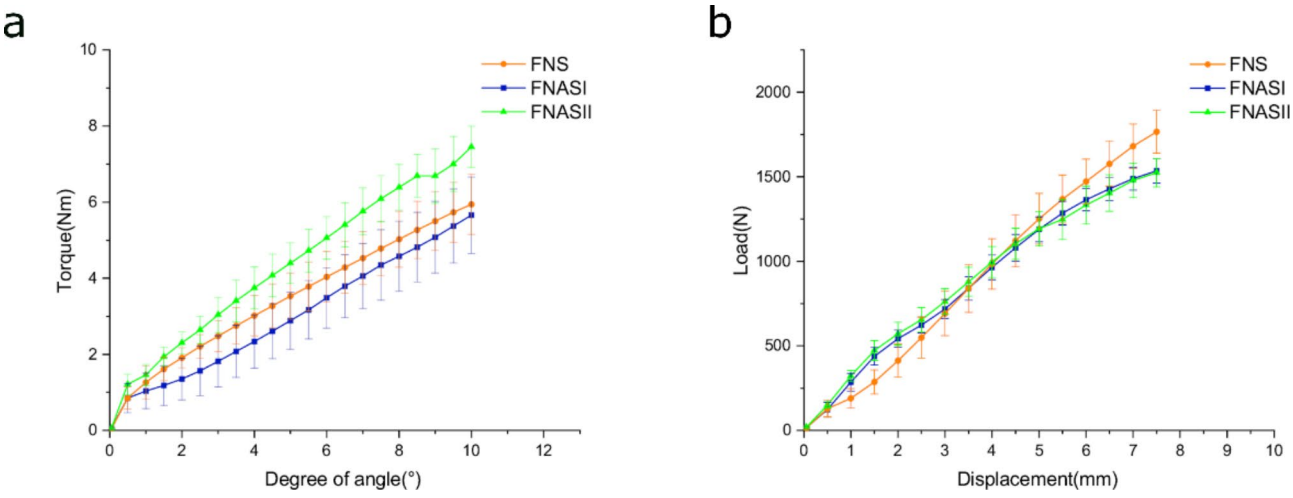

Fig. 5 Load-deformation curves of three fixation methods. (**a**) torque-angle curve; (**b**) load–displacement curve

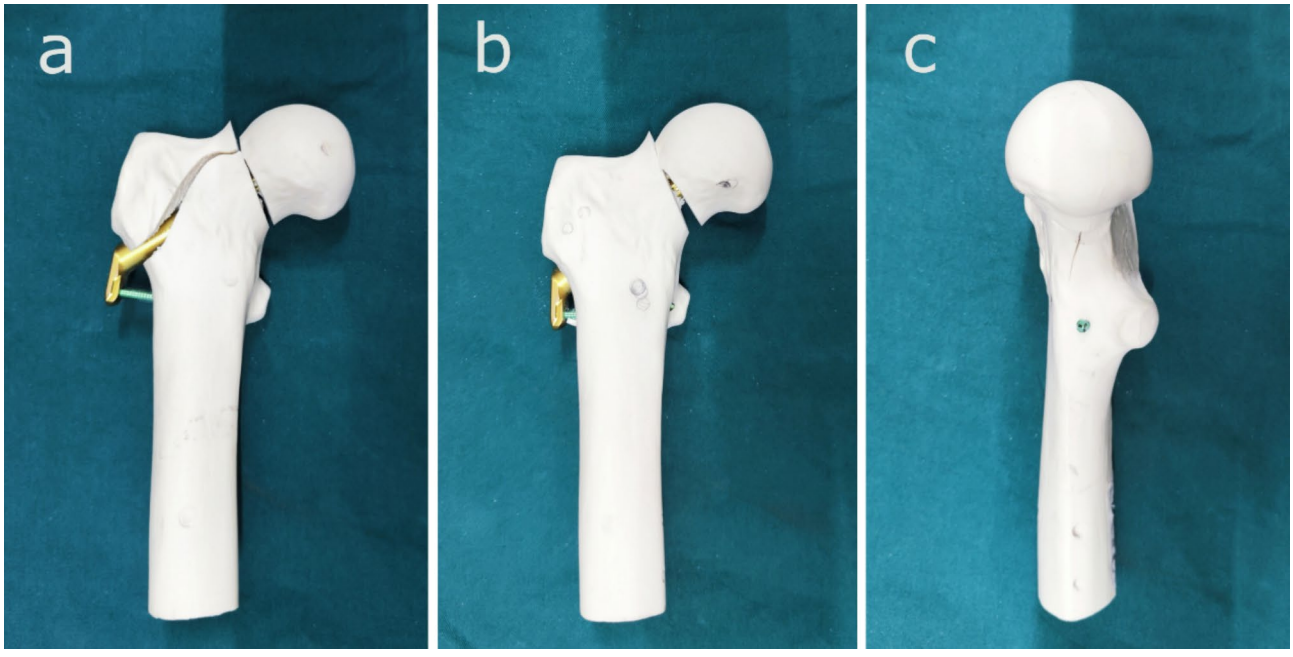

Fig. 6 Typical failure patterns of three fixation methods. (**a**) reverse oblique intertrochanteric femur fracture; (**b**) pull-out of the distal locking screw; (**c**) cleft on the calcar femorale

Table 2 Failure patterns of three fixation methods

Group	Failure patterns	No.
FNS	Pull-out of the distal locking screw	5
	Reverse oblique intertrochanteric femur fracture	1
FNAS I	Cleft on the calcar femorale	5
	Decrease on the load–displacement curve	1
FNAS II	Cleft on the calcar femorale	3
	Decrease on the load–displacement curve	3

to the twisting angle (θ), with the formula for torsional stiffness expressed as:

$$K_t = \frac{T}{\theta} \tag{1}$$

Torsional moment of inertia (J) is a geometrical property that quantifies a cross-section's resistance to twisting and can be expressed as:

$$J = \int (A)\, r^2 dA \tag{2}$$

In this equation: J is the torsional moment of inertia, r is the distance from a point on the cross-section to the axis of rotation, dA is an infinitesimal area element of the cross-section. Torsional stiffness can be related to torsional moment of inertia through the following formula:

$$K_t = \frac{GJ}{L} = \frac{G \int (A)\, r^2 dA}{L} \tag{3}$$

Where G is the material's shear modulus; J is the torsional moment of inertia; L is the length of the element. From this formula, it is evident that a larger torsional moment of inertia (J), assuming the shear modulus (G) and length (L) remain constant, indeed increases torsional stiffness (K_t). For FNS, FNAS I, and FNAS II, which are all made of titanium alloy with uniform specifications, the shear modulus (G) and length (L) are consistent across the groups. While r^2 value for FNAS II is larger due to its greater angle between the bolt and the anti-rotation screw, it is evident that the torsional stiffness (K_t) of FNAS II is higher than that of FNS and FNAS I. Since the angle of FNS and FNAS I is the same, their r^2 values are identical, meaning there is no difference in their torsional stiffness (K_t). This observation is in accordance with the biomechanical testing results.

Evidence from prior studies [16] suggested that polyaxial anchorage surpassed monoaxial fixation in preventing the rotation of the femoral head. A recent biomechanical study [17] showed that a novel internal fixation device, structurally similar to the Intertan nail but with screws positioned further from the femoral neck axis, significantly enhanced rotational stability compared to the Intertan nail, which aligned with our research findings. Therefore, irrespective of the impact of the fixation device's geometry on mechanical properties [18], the distance of the device from the rotation axis may be an important factor affecting its resistance to rotation.

Considering the turning point in the load–displacement curve in Fig. 5, the axial stiffness of both FNAS groups is higher than that of the FNS group before this turning point, which is approximately 800 to 1100 N load. The load at the turning point is about 140% of the weight of a 70 kg patient, which is sufficient to withstand the load of most activities in daily life [13]. Moreover, patients with femoral neck fractures are partially weight-bearing in the short term after internal fixation surgery, further reducing the load on the implants. This advantage is attributed to their anti-rotation screw, which provides buttressing and resistance in the calcar femorale and Ward's triangle area. The calcar femorale is a dense and vertical bone plate, acting as a buttress to improve implant stability, and the Ward's triangle refers to a relatively weak area between the primary and secondary compressive trabecular groups [7], thereby enhancing stability. After this turning point, the FNS's axial stiffness surpasses FNAS I and II, due to its anti-rotation screw near the primary compression trabeculae group, which effectively distributes and partly transfers stress to the femoral shaft.

Before the turning point, the bolt in each FNAS group is capable of transferring the stress from the femoral head to the femoral shaft. Both FNAS groups outperform the FNS group for reasons mentioned previously. As the load continues to increase, the bolt can no longer transfer all stress on its own. The anti-rotation screw in the FNS distributes the bolt's stress and transfers part of the stress. Although the anti-rotation screw in each FNAS group provides buttressing and resistance functions, its ability to transfer stress is weaker than that of the FNS group. This weakness is due to the screw's position being farther from the primary direction of stress transfer. Consequently, the mean axial stiffness of FNS is higher than that observed in both FNAS groups.

The failure mode of FNS, FNAS I, and FNAS II varies across the groups. Five cases of FNS (83.3%) are recorded with the pull-out of the distal locking screw, which is a typical failure pattern in accordance with a recent study [19]. The region of the distal locking screw is where stress concentrates, and this may induce subtrochanteric refracture [20], which is difficult to manage when there is already an implant in the femur. A catastrophic failure in one case of FNS (16.7%) occurs, which is a reverse oblique intertrochanteric femur fracture without the lateral femoral wall. The communication of the lateral femoral wall leads to complications like femoral head rotation and coxa vara [21]. A study stated a 22% reoperation rate

with lateral cortex fragmentation [22], which is unacceptable for patients who suffer a refracture. Regarding FNAS I, five cases (83.3%) exhibit a cleft of the calcar femorale, and one case (16.7%) reaches the failure criteria with a sudden decrease in load resistance observed on the load–displacement curve. For FNAS II, three cases show a cleft of the calcar femorale, and the other three cases demonstrate a decrease in the load–displacement curve. The crack of the calcar femorale often occurs as intraoperative fractures in cementless total hip arthroplasty (THA), which is usually managed by cerclage wires or cables [23]. Compared to the removal of internal fixation and reinsertion in the case of failure in the FNS group, the use of cerclage wires or cables in the FNAS groups represents a more minimally invasive and less traumatic surgery. The region where stress concentrates is the locking part of the bolt and the anti-rotation screw, which induces the cleft of the calcar femorale.

This study has several limitations. First, artificial composite bone is chosen for biomechanical analysis, which mimics the bone properties of young patients rather than those of the elderly. Since our study primarily focus on young patients with unstable femoral neck fracture, the conclusions may not be applicable to older patients. Second, the model do not simulate the muscles and ligaments of the femur, which play a crucial role in fracture stabilization. Finally, the model is only subjected to torsional and axial compression tests until failure. Further studies are required to validate the advantages and limitations of the FNS and FNAS in patients with osteoporosis.

Conclusion

This study has demonstrated that in unstable Pauwels III femoral neck fractures, the FNAS II enhances rotational and axial stability, which reduces the rates of cut-out of implants. Additionally, the failure modes of FNAS II are more manageable for reoperation compared to FNS. The results of the current study support the potential of FNAS II as an alternative option for treating unstable Pauwels III femoral neck fractures in young individuals.

Abbreviations

FNAS Femoral Neck Anti-rotation and Support System
FNS Femoral Neck System

Acknowledgements

We thank the Key Laboratory of Spine & Trauma Implant Devices of Chongqing Municipal Ministry of Industry and Information Technology for valuable help in our experiment.

Author contributions

Taiyou Wang &; Guangjian Wang: Conceptualization, Design and implement experiments, Methodology, Data curation, Writing; Fukang Zhu: Methodology, Data Analysis, Writing; Bo Qiao: Conceptualization, Writing, Supervision, Project administration, Funding acquisition.

Funding

This research was funded by the Chongqing Municipal Science and Technology Bureau (Grant No.cstc2020jscx-sbqwX0010).

Data availability

The data that support the findings of this study are available from the corresponding author upon reasonable request.

Declarations

Ethics approval and consent to participate

No ethical approval is required.

Consent for publication

Not applicable.

Competing Interests

The authors have no relevant financial or non-financial interests to disclose.

Author details

[1]Department of Orthopedics, The First Affiliated Hospital of Chongqing Medical University, 1 Youyi Rd, Chongqing 400010, P. R. China
[2]Orthopedic Laboratory of Chongqing Medical University, Chongqing 400010, P. R. China
[3]Department of Orthopedics, The People's Hospital of Rongchang District, Chongqing 402460, P. R. China

Received: 29 May 2024 / Accepted: 6 August 2024
Published online: 22 August 2024

References

1. Kanis JA, Odén A, McCloskey EV, Johansson H, Wahl DA, Cooper C. A systematic review of hip fracture incidence and probability of fracture worldwide. Osteoporos Int. 2012;23(9):2239–56.
2. Jiang X, Liang K, Du G, Chen Y, Tang Y, Geng K. Biomechanical evaluation of different internal fixation methods based on finite element analysis for Pauwels type III femoral neck fracture. Injury. 2022;53(10):3115–23.
3. Kuan FC, Hsu KL, Lin CL, Hong CK, Yeh ML, Su WR. Biomechanical properties of off-axis screw in Pauwels III femoral neck fracture fixation: bicortical screw construct is superior to unicortical screw construct. Injury. 2019;50(11):1889–94.
4. Luttrell K, Beltran M, Collinge CA. Preoperative decision making in the treatment of high-angle vertical femoral neck fractures in young adult patients. An expert opinion survey of the Orthopaedic Trauma Association's (OTA) membership. J Orthop Trauma. 2014;28(9):e221–5.
5. Liporace F, Gaines R, Collinge C, Haidukewych GJ. Results of internal fixation of Pauwels type-3 vertical femoral neck fractures. J Bone Joint Surg Am. 2008;90(8):1654–9.
6. Rajnish RK, Srivastava A, Rathod PM, Haq RU, Aggarwal S, Kumar P, et al. Does the femoral neck system provide better outcomes compared to cannulated screws fixation for the management of femoral neck fracture in young adults? A systematic review of literature and meta-analysis. J Orthop. 2022;32:52–9.
7. Sheehan SE, Shyu JY, Weaver MJ, Sodickson AD, Khurana B. Proximal femoral fractures: what the Orthopedic Surgeon wants to know. Radiographics. 2015;35(5):1563–84.
8. Kemker B, Magone K, Owen J, Atkinson P, Martin S, Atkinson T. A sliding hip screw augmented with 2 screws is biomechanically similar to an inverted triad of cannulated screws in repair of a Pauwels type-III fracture. Injury. 2017;48(8):1743–8.
9. Bartonícek J. Pauwels' classification of femoral neck fractures: correct interpretation of the original. J Orthop Trauma. 2001;15(5):358–60.
10. Brattgjerd JE, Steen H, Strømsøe K. Increased stability by a novel femoral neck interlocking plate compared to conventional fixation methods. A biomechanical study in synthetic bone. Clin Biomech (Bristol Avon). 2020;76:104995.
11. Zdero R, Keast-Butler O, Schemitsch EH. A biomechanical comparison of two triple-screw methods for femoral neck fracture fixation in a synthetic bone model. J Trauma. 2010;69(6):1537–44.

12. Ragnarsson JI, Kärrholm J. Factors influencing postoperative movement in displaced femoral neck fractures: evaluation by conventional radiography and stereoradiography. J Orthop Trauma. 1992;6(2):152–8.
13. Bergmann G, Deuretzbacher G, Heller M, Graichen F, Rohlmann A, Strauss J, et al. Hip contact forces and gait patterns from routine activities. J Biomech. 2001;34(7):859–71.
14. Nie S, Li M, Ji H, Li Z, Li W, Zhang H, et al. Biomechanical comparison of medial sustainable nail and proximal femoral nail antirotation in the treatment of an unstable intertrochanteric fracture. Bone Joint Res. 2020;9(12):840–7.
15. Gosiewski JD, Holsgrove TP, Gill HS. The efficacy of rotational control designs in promoting torsional stability of hip fracture fixation. Bone Joint Res. 2017;6(5):270–6.
16. Santoni BG, Nayak AN, Cooper SA, Smithson IR, Cox JL, Marberry ST, et al. Comparison of femoral Head Rotation and Varus Collapse between a single lag Screw and Integrated Dual Screw Intertrochanteric hip fracture fixation device using a cadaveric hemi-pelvis Biomechanical Model. J Orthop Trauma. 2016;30(4):164–9.
17. Park DH, Seo YC, Kwon YU, Jung SH, Yoo SJ. Biomechanical comparative study for Osteosynthesis of Pauwels Type III femoral Neck fractures: Conventional devices versus Novel fixed Angle devices. Hip Pelvis. 2022;34(1):35–44.
18. Brattgjerd JE, Loferer M, Niratisairak S, Steen H, Strømsøe K. Increased torsional stability by a novel femoral neck locking plate. The role of plate design and pin configuration in a synthetic bone block model. Clin Biomech (Bristol Avon). 2018;55:28–35.
19. Moon JK, Lee JI, Hwang KT, Yang JH, Park YS, Park KC. Biomechanical comparison of the femoral neck system and the dynamic hip screw in basicervical femoral neck fractures. Sci Rep. 2022;12(1):7915.
20. Lourenço BC, Amorim-Barbosa T, Lemos C, Rodrigues-Pinto R. Risk factors for refracture after proximal femur fragility fracture. Porto Biomed J. 2023;8(2):e207.
21. Polat G, Akgül T, Ekinci M, Bayram S. A biomechanical comparison of three fixation techniques in osteoporotic reverse oblique intertrochanteric femur fracture with fragmented lateral cortex. Eur J Trauma Emerg Surg. 2019;45(3):499–505.
22. Palm H, Jacobsen S, Sonne-Holm S, Gebuhr P. Integrity of the lateral femoral wall in intertrochanteric hip fractures: an important predictor of a reoperation. J Bone Joint Surg Am. 2007;89(3):470–5.
23. Mei J, Pang L, Jiang Z. Strategies for managing the destruction of calcar femorale. BMC Musculoskelet Disord. 2021;22(1):460.

Publisher's Note